SUPPORTING INFORMATION

Combined experimental and computational studies of pyrazinamide and nicotinamide in the context of crystal engineering and thermodynamics

Katarzyna N. Jarzembska,[a,b‡] Anna A. Hoser,[a‡] Radosław Kamiński,[a,b*]
Anders Ø. Madsen,[c] Krzysztof Durka,[d] Krzysztof Woźniak[a]

[a] Department of Chemistry, University of Warsaw, Pasteura 1, 02-093 Warszawa, Poland

[b] Department of Chemistry, University at Buffalo, The State University of New York, Buffalo, New York 14260-3000, USA

[c] Department of Chemistry, University of Copenhagen, Universitetparken 5, 2100 Copenhagen, Denmark

[d] Department of Chemistry, Warsaw University of Technology, Noakowskiego 3, 00-664, Warszawa, Poland

* Corresponding author: Radosław Kamiński (rkaminski@chem.uw.edu.pl)

‡ Both authors contributed equally to this work

1S. Multipole refinement details

Multipole refinements were performed in the *MOPRO* suite (Guillot *et al.*, 2001; Jelsch *et al.*, 2005) combined with the latest version of the University at Buffalo Data Bank (UBDB) (Jarzembska & Dominiak, 2012), based on the Hansen-Coppens multipole model (Hansen & Coppens, 1978). Refinement was based on F, and only the reflections fulfilling the $I \geq 3\sigma(I)$ condition were taken into account. The statistical weights were used (*i.e.* for i-th reflection $w_i = 1/\sigma_i^2$). Initial atomic coordinates, x, y, and z, and anisotropic displacement parameters (U_{ij}'s) for each atom were taken from the spherical refinement stage, whereas initial multipolar and contraction-expansion parameters were transferred from UBDB with the aid of the *LSDB* program (Volkov *et al.*, 2004; Jarzembska & Dominiak, 2012). Additionally, the X–H bond lengths (X = non-hydrogen atom) were standardised to neutron-normalised distances according to the values tabulated by Allen & Bruno ($d_{\mathrm{C-H}}$ = 1.083 Å, $d_{\mathrm{N-H}}$ = 1.010 Å) (Allen & Bruno, 2010; Allen, 2002). The *MOPRO* program allows for the application of specific restraints during the refinement. Therefore, in the initial stage, the hydrogen atom U_{iso} parameters (*i.e.* isotropic thermal parameters) were restrained to the value of $1.5 \cdot U_{\mathrm{eq}}^{\mathrm{X}}$ with σ = 0.01 (where the appropriate restraint weight is equal to $1/\sigma^2$). In the final stage refinements, the derivation of anisotropic hydrogen atom ADPs was carried out using the *SHADE* server (Munshi *et al.*, 2008; Madsen, 2006). The X–H bond lengths were restrained to neutron-normalised distances with σ = 0.001. This approach has recently been successfully tested in a variety of studies, providing results comparable with the corresponding theoretical periodic computations and neutron studies (Kamiński *et al.*, 2014; Jarzembska *et al.*, 2012). The multipole expansion was truncated at the hexadecapole (l_{max} = 3) and quadrupole (l_{max} = 2) levels for all non-hydrogen and hydrogen atoms, respectively. All κ' parameters were kept fixed at the UBDB-transferred values.

All atomic deformation density functions were subjected to the local symmetry constraints, suggested initially by the *LSDB* program. Specifically, for hydrogen atoms only the bond-directed dipole and octupole populations (*i.e.*, P_{10} and P_{20}) were refined. Such an approach has recently been tested in the case of oxalic acid molecule, and has been shown to provide results within the limit of the Hansen-Coppens formalism precision available nowadays (Kamiński *et al.*, 2014). It is worth noting that the importance of the proper treatment of local symmetry constraints and restraints in

charge density studies has been highlighted in a number of recent works (Zarychta *et al.*, 2007; Paul *et al.*, 2011; Poulain-Paul *et al.*, 2012).

Finally, the general strategy for refinement was as follows: (i) scale factor (which was also refined in all other stages); (ii) atomic coordinates; (iii) atomic coordinates and ADPs; (iv) *SHADE* estimation of anisotropic hydrogen atom ADPs (which was also updated in-between other stages until convergence); (v) multipole parameters in a stepwise manner; (vi) all population and structural parameters simultaneously; (vii) block refinement of no. (vi) and κ parameters; (viii) all parameters simultaneously.

The refinement resulted in models with very flat and almost featureless residual density distribution ($\Delta\varrho_{\mathrm{res}}$ = −0.14/+0.16 e·Å^{-3}, and $\Delta\varrho_{\mathrm{res}}$ = −0.12/+0.13 e·Å^{-3} for $\boldsymbol{\beta}_{\mathbf{PYRA}}$ and $\boldsymbol{\alpha}_{\mathbf{NICO}}$, respectively). Residual density properties were evaluated with the *JNK2RDA* program (Meindl & Henn, 2008). All final refinement statistics are summarized in Table 1 (main article). CIF files for both refinements are available as the Supporting Information, or can be retrieved from the Cambridge Structural Database (Allen, 2002) (deposition numbers: CCDC 991917 & CCDC 991918).

2S. Theoretical computations and entropy estimation details

2S.1. Cohesive and dimer interaction energies. The *CRYSTAL* package (Dovesi *et al.*, 2005; Dovesi *et al.*, 2009) (version: *CRYSTAL09*) was used for the evaluation of crystal cohesive energy values and dimer interaction energies. B3LYP/pVTZ level of theory (Becke, 1988; Lee *et al.*, 1988; Dunning, 1989; Schäfer *et al.*, 1994) was employed with both Grimme dispersion (Grimme, 2004, 2006) and BSSE corrections (Boys & Bernardi, 1970). Ghost atoms were selected up to 5 Å distance from the considered molecule in a crystal lattice, and were used for the BSSE estimation. The evaluation of Coulomb and exchange series was controlled by five thresholds, set arbitrarily to the values of 10^{-7}, 10^{-7}, 10^{-7}, 10^{-7}, 10^{-25}. Shrinking factor was equal to 8, which refers to 170 **k**-points in the irreducible Brillouin zone and assures the full convergence of the total energy. The cohesive energy (E_{coh}) was calculated as follows:

$$E_{\mathrm{coh}} = \frac{1}{Z} E_{\mathrm{bulk}} - E_{\mathrm{mol}}$$

where E_{bulk} is the total energy of a system (calculated per unit cell) and E_{mol} is the energy of a molecule extracted from the bulk. Z stands for the number of molecules in the unit cell. The input files were prepared using the *CLUSTERGEN* program (Kamiński *et al.*, 2013).

Additionally, the cohesive energy and dimer interaction energy values were estimated with the aid of the *PIXEL* approach (Gavezzotti, 2003b, 2002, 2003a, 2005) at the MP2/6-31G** level of theory (Møller & Plesset, 1934; Krishnan *et al.*, 1980), which enabled total energy decomposition into electrostatic, polarization, dispersion and repulsion contributions.

2S.2. Entropy estimation. In order to evaluate crystal vibrational entropy we estimated in different ways part of entropy related to high-frequency modes and part related to low-frequency lattice vibrations.

Vibrational entropy associated with the low-frequency modes, was evaluated on the base of Madsen & Larsen approach. First, TLS analysis was conducted and related frequencies (and some estimated standard uncertainties, based on the standard uncertainties given for the eigenvalues of the TLS-fit matrix in the *THMA* program) were computed. Next, on the basis of such evaluated frequencies, the vibrational entropy of crystals as a function of temperature was calculated as a sum of the contributions from each oscillator:

$$S_{\mathrm{TLS}}(T) = R\sum_i \left(\frac{h\nu_i}{k_{\mathrm{B}}T}\left[\exp\left(\frac{h\nu_i}{k_{\mathrm{B}}T}\right)-1\right]^{-1} - \ln\left[1-\exp\left(-\frac{h\nu_i}{k_{\mathrm{B}}T}\right)\right]\right)$$

where R is the gas constant, k_{B} is the Boltzmann constant, and ν_i is a frequency of a given i-th oscillator. Following the above procedure, vibrational entropy was estimated for $\boldsymbol{\beta}_{\mathbf{PYRA}}$ and $\boldsymbol{\alpha}_{\mathbf{NICO}}$, on the basis of the collected high-resolution X-ray diffraction data with different resolution cut-offs and approaches of obtaining ADPs.

The frequencies related to the high-frequency vibrational modes were calculated using the *CRYSTAL* code. First, to assure that the geometries used for the frequency calculations reached stationary points on the potential energy surface (PES), the geometry optimizations were performed. The atomic coordinates were optimized, whereas the lattice constants were kept fixed. Molecular geometries obtained after *CRYSTAL* calculations were very similar to those from experiment (Figure 2S; root-mean-square-deviation (RMSD) between experimental and optimised molecular geometry equals 0.018 Å for nicotinamide, whereas 0.027 Å for pyrazinamide). Subsequently, high-frequency vibrational modes were computed and used to estimate the 'internal' contribution to the crystal entropy (S_{CRY}). The geometry optimizations and frequency calculations were carried out at the B3LYP/6-31G** level of theory for both compounds.

3S. Additional figures

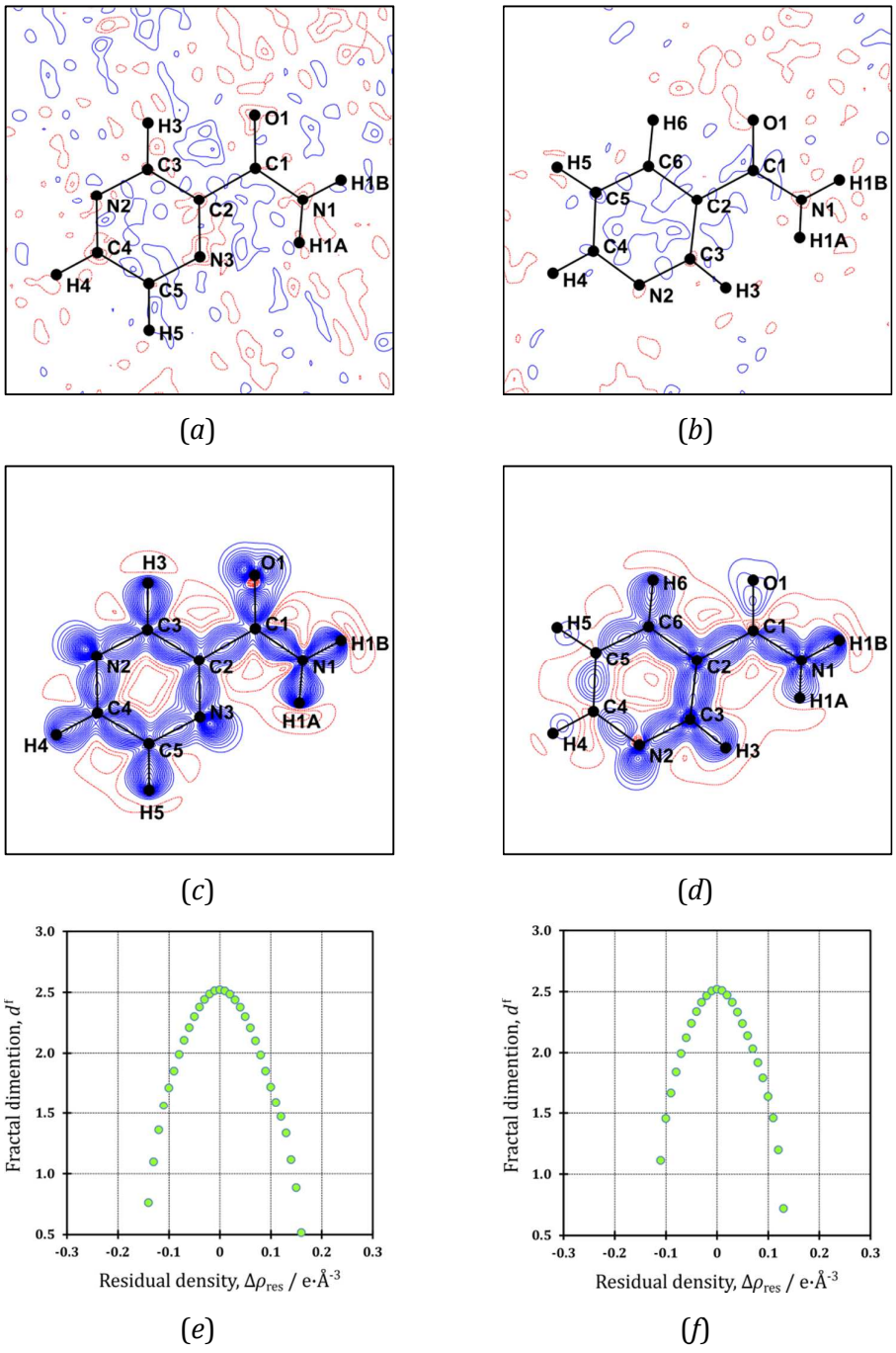

Figure 1S. Residual (*a*,*b*) and static deformation (*c*,*d*) density maps (contours at 0.05 e·Å^{-3}; blue solid lines – positive contours, red dashed lines – negative contours). Residual density fractal plots (*e*,*f*). Left panels: $\boldsymbol{\beta}_{\mathbf{PYRA}}$; Right panels: $\boldsymbol{\alpha}_{\mathbf{NICO}}$ (the molecule is not completely flat).

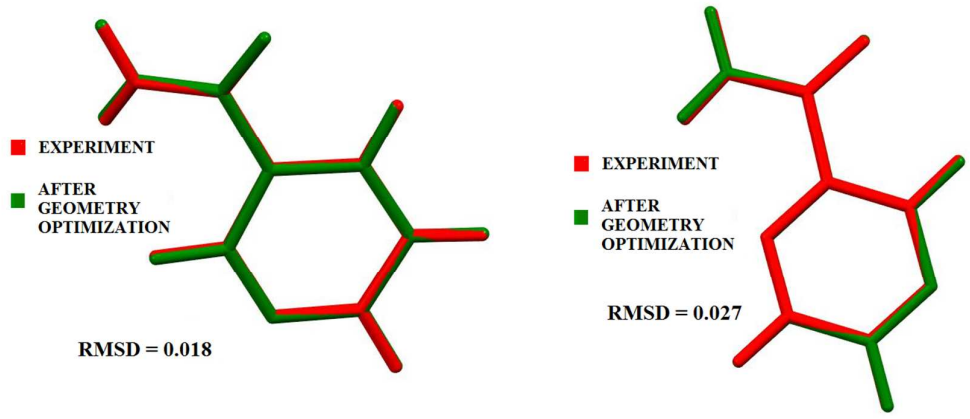

(*a*) (*b*)

Figure 2S. Overlay of molecular geometries obtained from the experiment and after the geometry optimization for (*a*) $\boldsymbol{\alpha_{NICO}}$ (*b*) $\boldsymbol{\beta_{PYRA}}$ (RMSD – root-mean-square deviation; given in Å).

4S. Additional references

Allen, F. H. (2002). *Acta Cryst.* **B58**, 380-388.

Allen, F. H. & Bruno, I. J. (2010). *Acta Cryst.* **B66**, 380-386.

Becke, A. D. (1988). *Phys. Rev. A* **38**, 3098-3100.

Boys, S. F. & Bernardi, F. (1970). *Mol. Phys.* **19**, 553-566.

Dovesi, R., Civalleri, B., Orlando, R., Roetti, C. & Saunders, V. R. (2005). *Rev. Comput. Chem.* **21**, 1-125.

Dovesi, R., Saunders, V. R., Roetti, C., Orlando, R., Zicovich-Wilson, C. M., Pascale, F., Civalleri, B., Doll, K., Harrison, N. M., Bush, I. J., D'Arco, P. & Llunell, M. (2009). *CRYSTAL09*. University of Torino, Torino.

Dunning, T. H. (1989). *J. Chem. Phys.* **90**, 1007-1023.

Gavezzotti, A. (2002). *J. Phys. Chem. B* **106**, 4145-4154.

Gavezzotti, A. (2003a). *CrystEngComm* **5**, 429-438.

Gavezzotti, A. (2003b). *J. Phys. Chem. B* **107**, 2344-2353.

Gavezzotti, A. (2005). *J. Chem. Theor. Comput.* 834-840.

Grimme, S. (2004). *J. Comput. Chem.* **25**, 1463-1473.

Grimme, S. (2006). *J. Comput. Chem.* **27**, 1787-1799.

Guillot, B., Viry, L., Guillot, R., Lecomte, C. & Jelsch, C. (2001). *J. Appl. Cryst.* **34**, 214-223.

Hansen, N. K. & Coppens, P. (1978). *Acta Cryst.* **A34**, 909-921.

Jarzembska, K. N. & Dominiak, P. M. (2012). *Acta Cryst.* **A68**, 139-147.

Jarzembska, K. N., Kubsik, M., Kamiński, R., Woźniak, K. & Dominiak, P. M. (2012). *Cryst. Growth Des.* **12**, 2508-2524.

Jelsch, C., Guillot, B., Lagoutte, A. & Lecomte, C. (2005). *J. Appl. Cryst.* **38**, 38-54.

Kamiński, R., Domagała, S., Jarzembska, K. N., Hoser, A. A., Sanjuan-Szklarz, W. F., Gutmann, M. J., Makal, A., Malińska, M., Bąk, J. M. & Woźniak, K. (2014). *Acta Cryst.* **A70**, 72-91.

Kamiński, R., Jarzembska, K. N. & Domagała, S. (2013). *J. Appl. Cryst.* **46**, 540-534.

Krishnan, R., Binkley, J. S., Seeger, R. & Pople, J. A. (1980). *J. Chem. Phys.* **72**, 650-654.

Lee, C., Yang, W. & Parr, R. G. (1988). *Phys. Rev. B* **37**, 785-789.

Madsen, A. Ø. (2006). *J. Appl. Cryst.* **39**, 757-758.

Meindl, K. & Henn, J. (2008). *Acta Cryst.* **A64**, 404-418.

Møller, C. & Plesset, M. S. (1934). *Phys. Rev.* **46,** , 618-622.

Munshi, P., Madsen, A. Ø., Spackman, M. A., Larsen, S. & Destro, R. (2008). *Acta Cryst.* **A64**, 465-475.

Paul, A., Kubicki, M., Jelsch, C., Durand, P. & Lecomte, C. (2011). *Acta Cryst.* **B67**, 365-378.

Poulain-Paul, A., Nassour, A., Jelsch, C., Guillot, B., Kubicki, M. & Lecomte, C. (2012). *Acta Cryst.* **A68**, 715-728.

Schäfer, A., Huber, C. & Alrichs, R. (1994). *J. Chem. Phys.* **100**, 5829-5835.

Volkov, A., Li, X., Koritsanszky, T. & Coppens, P. (2004). *J. Phys. Chem. A* **108**, 4283-4300.

Zarychta, B., Pichon-Pesme, V., Guillot, B., Lecomte, C. & Jelsch, C. (2007). *Acta Cryst.* **A63**, 108.